Target Detection in Interference and Non-Gaussian Sea Clutter with Limited Training Data

Hongzhi Guo, Haoqi Wu, Xinghe Li, Zhihang Wang, Zishu He, and Ziyang Cheng
School of Information and Communication Engineering,
University of Electronic Science and Technology of China, Chengdu 611731, Sichuan, China.
Email: hongz_guo@126.com; haoqi_wu1017@163.com; zhihang_w@uestc.edu.cn; zshe@uestc.edu.cn

***Abstract*—This paper deals with the problem of subspace detection in structured interference plus non-Gaussian sea clutter. The non-Gaussian sea clutter is modelled as the inverse Gaussian texture compound Gaussian (IG-CG) distribution. We project the detection problem onto the interference-orthogonal subspace by exploiting the interference cancellation before detection (ICBD) method. We design three novel detectors based on the two-step generalized likelihood ratio test (GLRT), Rao, and Wald tests. The Monte Carlo experiments demonstrate the novel subspace detectors achieve higher performance gain than the comparison detectors. The Numerical examples show that the proposed detector has good anti-interference performance and can operate in scenarios with insufficient training data.**

***Index Terms*—Subspace detection, Non-Gaussian clutter, Subspace interference, Limited training data**

I. Introduction

Target detection in non-homogenous sea clutter with unknown clutter covariance matrix (CM) has been widely studied in the fields of radar, sonar, and remote sensing [1], [2]. Based on the two-step generalized likelihood ratio test (GLRT), the adaptive matched filter (AMF) detector is proposed in the Gaussian environment [3]. As the rank-1 signal cannot accurately describe the characteristics of the target, the detector for the Multirank signal is considered in [4], which is the matched subspace detector (MSD).

With the increase of radar resolution and the decrease of radar electromagnetic wave grazing angle, the sea clutter may exhibit heavy-tailed non-Gaussian distribution. The subspace detection problem in K distribution sea clutter has been studied in [5]. The detectors for polarimetric radar, which are constant false alarm rate (CFAR) tests with respect to (w.r.t) the speckle covariance matrix, are derived based on the two-step maximum *a posteriori* (MAP) GLRT, Rao, and Wald tests [6]. The adaptive detection problem in compound Gaussian distribution with lognormal texture is considered in [7] for coherent high-resolution radar. As the inverse Gaussian texture compound Gaussian (IG-CG) sea clutter may fit the measured sea clutter well [8], the subspace detection of distributed targets in the inverse Gaussian sea clutter is investigated in [9].

However, the interference, which may seriously affect the detection performance of the detectors, may occur in real applications. A unifying framework for radar detection in structured interference is proposed in [10]. The subspace detection of the subspace signal embedded in structured interference plus Gaussian interference, which can be solved by the principle of invariance, is investigated in [11]. The subspace detectors for targets in IG-CG clutter with interference are proposed in [12].

Most of the detectors mentioned above do not consider the situation of limited training data, which may lead to inaccurate or even singular covariance matrix estimation. The authors in [13] consider the radar systems using a symmetric interval linear array with constant pulse repetition interval to improve the detection performance. In [14], the detection problem in the compound Gaussian sea clutter is studied with persymmetric speckle covariance matrix. Moreover, the prior information of the speckle covariance matrix can be exploited to improve the detection performance for radar targets [15].

The detectors above either only focus on the interference that only occurs in the cell under test (CUT) or insufficient training data, as the subspace interference may exist in training data units [16], especially in the situation of limited training data [17]. In [17], the authors consider the problem of target detection in structured interference in Gaussian environment with limited training data.

In this paper, we consider the detection problem of subspace detection in structured interference plus IG-CG sea clutter. Besides, we design three novel subspace detectors, which can operate in the limited training data situation. We verify the detection performance of the proposed detectors outperforms the competitors in the simulated and measured sea clutter data.

Notations: We use the light face b, lower case bold face $\mathbf{b}$, and upper case bold face $\mathbf{B}$ to denote scalar, vector, and matrix, respectively. $(\cdot)^H$ is the conjugate transpose operator. $E(\cdot)$ and $\det(\cdot)$ are the operations of expectation and determinant. The inverse of $\mathbf{B}$ is given by $\mathbf{B}^{-1}$. $\mathbb{C}$ is the set of complex numbers. $\mathrm{Tr}(\cdot)$ is the trace of the matrix.

II. Problem Formulation and Model

Assume that the radar system receives signals from N antenna senses. The N-dimensional vector $\mathbf{z}_0 \in \mathbb{C}^{N\times 1}$ denotes the primary data, which is called cell under test (CUT). The secondary data (i.e. training data) $\mathbf{z}_k \in \mathbb{C}^{N\times 1}$ represent the k-th range cell adjacent to the CUT. Therefore, the binary

This work was supported in part by the National Natural Science Foundation of China under Grant 62301124, Grant 62031007, and Grant 62231006; and in part by the Sichuan Province Science and Technology Plan under Grant 2023ZHJY0011.

hypothesis test of the target detection in subspace interference and non-Gaussian sea clutter is given by:

$$\begin{cases} H_0: \begin{cases} \mathbf{z}_0 = \mathbf{J}\boldsymbol{\varphi} + \mathbf{c}_0 \\ \mathbf{z}_k = \mathbf{J}\boldsymbol{\varphi} + \mathbf{c}_k, k = 1, \cdots, K \end{cases} \\ H_1: \begin{cases} \mathbf{z}_0 = \mathbf{H}\boldsymbol{\beta} + \mathbf{J}\boldsymbol{\varphi} + \mathbf{c}_0 \\ \mathbf{z}_k = \mathbf{J}\boldsymbol{\varphi} + \mathbf{c}_k, k = 1, \cdots, K \end{cases} \end{cases} \tag{1}$$

where where the hypothesis H_0 denotes the absence of the target, and the hypothesis H_1 represents the presence of the target. $\mathbf{H}\boldsymbol{\beta}$ and $\mathbf{J}\boldsymbol{\varphi}$ denote the signal and the interference, respectively. The columns of the subspace signal matrix $\mathbf{H} \in \mathbb{C}^{N\times t}$ span the signal subspace $\langle \mathbf{H} \rangle$, and the columns of the interference signal matrix $\mathbf{J} \in \mathbb{C}^{N\times p}$ span the interference subspace $\langle \mathbf{J} \rangle$. We hold $\boldsymbol{\beta} = b\boldsymbol{\beta}'$ and $\boldsymbol{\varphi} = a\boldsymbol{\varphi}'$, where the unknown N-dimensional vectors $\boldsymbol{\beta}'$ and $\boldsymbol{\varphi}'$ stand for the normalized coordinate of the signal and interference in $\langle \mathbf{H} \rangle$ and $\langle \mathbf{J} \rangle$, respectively. b and a denote the amplitude of the target signal and the interference. The full-column-rank matrix $\mathbf{H}$ and $\mathbf{J}$ are known in advance, $t + p \leqslant K$. $\mathbf{c}_0$ and $\mathbf{c}_k$ denote the sea clutter in the CUT and the k-th range cell adjacent to the CUT.

We set $\mathbf{c}_0 = \tau\sqrt{\mathbf{g}_0}$ and $\mathbf{c}_k = \tau\sqrt{\mathbf{g}_k}$, where $\mathbf{g}_0$ and $\mathbf{g}_k$ represent the speckle component. $\mathbf{g}_0$ and $\mathbf{g}_k$ are the zero-mean complex Gaussian vector with the unknown covariance matrix $\mathbf{R}_0$. The probability density function (PDF) of the texture component τ in the compound Gaussian sea clutter can be modelled by the inverse Gaussian distribution as follows:

$$f(\tau) = \sqrt{\frac{\lambda}{2\pi}}\tau^{-\frac{3}{2}} \exp\left[-\frac{\lambda}{2\mu^2\tau}(\tau - \mu)^2\right] \tag{2}$$

where λ and μ denote the shape parameter and the scale parameter of the inverse Gaussian distribution. Thus, the clutter covariance matrix can be expressed as $\mathbf{M}_0 = \tau\mathbf{R}_0$.

When the interference occupies several range cells with slowly varying [17], the interference both exists in CUT and training data in the problem (1). However, the interference in the training data only exists in a few range cells close to the CUT, which indicates the training data is limited (i.e. $K < N$). Therefore, the conventional detectors in [3], [4], [7], [9], [12] may lose effectiveness in compound Gaussian sea clutter.

We exploit the interference cancellation before detection (ICBD) method in compound Gaussian sea clutter. We define $\mathbf{J} = \mathbf{U}_1\mathbf{J}_1$, where $\mathbf{U}_1 = \mathbf{J}(\mathbf{J}^H\mathbf{J})^{-1/2}$, $\mathbf{J}_1 = (\mathbf{J}^H\mathbf{J})^{1/2}$. And $\mathbf{U}_1$ share the same range space with $\mathbf{J}$. We further define the unitary matrix $\mathbf{U} = [\mathbf{U}_1, \mathbf{U}_2]$, where $\mathbf{U}_2$ is a $N \times (N - p)$-dimensional column unitary matrix. And we note that $\mathbf{U}_2$ lies in the null space of the interference matrix $\mathbf{J}$. Thus, we exploit $\mathbf{U}_2^H$ multiplied (1) from the left, we obtain

$$\begin{cases} H_0: \begin{cases} \mathbf{x}_0 = \mathbf{n}_0 \\ \mathbf{x}_k = \mathbf{n}_k, k = 1, \cdots, K \end{cases} \\ H_1: \begin{cases} \mathbf{x}_0 = \mathbf{S}\boldsymbol{\beta} + \mathbf{n}_0 \\ \mathbf{x}_k = \mathbf{n}_k, k = 1, \cdots, K \end{cases} \end{cases} \tag{3}$$

where $\mathbf{x}_0 = \mathbf{U}_2^H\mathbf{z}_0, \mathbf{x}_k = \mathbf{U}_2^H\mathbf{z}_k, \mathbf{n}_0 = \mathbf{U}_2^H\mathbf{c}_0, \mathbf{n}_k = \mathbf{U}_2^H\mathbf{c}_k, \mathbf{S} = \mathbf{U}_2^H\mathbf{H}$. The covariance matrix of $\mathbf{n}_0$ and $\mathbf{n}_k$ are $\mathbf{M} = \tau\mathbf{R}$, where the novel speckle covariance matrix (CM) is $\mathbf{R} = \mathbf{U}_2^H\mathbf{R}_0\mathbf{U}_2$.

Therefore, the conditional PDF of $\mathbf{x}_0$ under hypothesis H_1 is given by:

$$f_1(\mathbf{x}_0 | \tau, \boldsymbol{\beta}, \mathbf{R}) = \frac{\exp\left[-\frac{1}{\tau}(\mathbf{x}_0 - \mathbf{S}\boldsymbol{\beta})^H\mathbf{R}^{-1}(\mathbf{x}_0 - \mathbf{S}\boldsymbol{\beta})\right]}{\pi^N\tau^N|\mathbf{R}|} \tag{4}$$

The conditional PDF of $\mathbf{x}_0$ under hypothesis H_0 can be expressed as follows:

$$f_0(\mathbf{x}_0 | \tau, \mathbf{R}) = \frac{1}{\pi^N\tau^N|\mathbf{R}|}\exp\left[-\frac{1}{\tau}\mathbf{x}_0^H\mathbf{R}^{-1}\mathbf{x}_0\right] \tag{5}$$

III. Design of proposed subspace detectors

In this section, we derive three subspace detectors based on two-step GLRT, the Rao and Wald tests.

A. ICBD-GLRT subspace detector

In the first step, we assume that the speckle CM $\mathbf{R}$ is known, and the GLRT criterion for (3) is given by:

$$\frac{\max_{\boldsymbol{\beta}} \int_0^{+\infty} f_1(\mathbf{x}_0 | \boldsymbol{\beta}, \tau) f(\tau) d\tau}{\int_0^{+\infty} f_0(\mathbf{x}_0 | \tau) f(\tau) d\tau} \underset{H_0}{\overset{H_1}{\gtrless}} \xi \tag{6}$$

where ξ denotes the detection thresholds. Then, we calculate the maximum likelihood (ML) estimate of $\boldsymbol{\beta}$ as follows:

$$\hat{\boldsymbol{\beta}} = (\mathbf{S}^H\mathbf{R}^{-1}\mathbf{S})^{-1}\mathbf{S}^H\mathbf{R}^{-1}\mathbf{x}_0 \tag{7}$$

According to (7) and the m-order modified Bessel function of the second kind, the numerator and denominator of (6) under H_q hypothesis is given by:

$$\begin{aligned} \int_0^{+\infty} f_q(\mathbf{x}_0 | \boldsymbol{\beta}, \tau) f(\tau) d\tau = & \frac{\sqrt{2\lambda}e^{\lambda/\mu}}{(\mu\pi)^{N+1/2}|\mathbf{R}|} \\ & \times \left(1 + \frac{2T_q}{\lambda}\right)^{-\frac{N}{2}-\frac{1}{4}} K_{N+\frac{1}{2}}\left(\frac{\lambda}{\mu}\sqrt{1 + \frac{2T_q}{\lambda}}\right) \end{aligned} \tag{8}$$

where $T_1 = \bar{\mathbf{x}}_0^H\mathbf{P}_{\bar{\mathbf{S}}}^{\perp}\bar{\mathbf{x}}_0, \bar{\mathbf{x}}_0 = \mathbf{R}^{-1/2}\mathbf{x}_0, \bar{\mathbf{S}} = \mathbf{R}^{-1/2}\mathbf{S}, \mathbf{P}_{\bar{\mathbf{S}}} = \bar{\mathbf{S}}(\bar{\mathbf{S}}^H\bar{\mathbf{S}})^{-1}\bar{\mathbf{S}}^H, \mathbf{P}_{\bar{\mathbf{S}}}^{\perp} = \mathbf{I}_N - \mathbf{P}_{\bar{\mathbf{S}}}, T_0 = \bar{\mathbf{x}}_0^H\bar{\mathbf{x}}_0$. And m-order modified Bessel function of the second kind is given by:

$$K_m(x) = \frac{1}{2}\left(\frac{x}{2}\right)^m \int_0^{+\infty} t^{-(m+1)} \exp\left(-t - \frac{x^2}{4t}\right) dt \tag{9}$$

In the second step, we estimate the speckle CM $\mathbf{R}$ by exploiting the fixed point (FP) covariance estimator as [18]:

$$\hat{\mathbf{R}}_{\text{FP}}^{(o+1)} = \frac{N}{K}\sum_{k=1}^{K} \frac{\mathbf{x}_k\mathbf{x}_k^H}{\mathbf{x}_k^H\left[\hat{\mathbf{R}}_{\text{FP}}^{(o)}\right]^{-1}\mathbf{x}_k} \tag{10}$$

where o is the iterations. And we set the identity matrix as the initial estimation.

Substituting (8) and (10) into (6), we obtain the ICBD-based subspace detector by exploiting GLRT in compound Gaussian

sea clutter with inverse Gaussian texture (ICBD-GLRT-IG) as follows:

$$\frac{\left(1+\frac{2\hat{T}_1}{\lambda}\right)^{-\frac{N}{2}-\frac{1}{4}} K_{N+\frac{1}{2}}\left(\frac{\lambda}{\mu}\sqrt{1+\frac{2\hat{T}_1}{\lambda}}\right)}{\left(1+\frac{2\hat{T}_0}{\lambda}\right)^{-\frac{N}{2}-\frac{1}{4}} K_{N+\frac{1}{2}}\left(\frac{\lambda}{\mu}\sqrt{1+\frac{2\hat{T}_0}{\lambda}}\right)} \underset{H_0}{\overset{H_1}{\gtrless}} \xi \tag{11}$$

where $\hat{T}_1 = \tilde{\mathbf{x}}_0^H \mathbf{P}_{\tilde{\mathbf{S}}}^{\perp} \tilde{\mathbf{x}}_0, \hat{T}_0 = \tilde{\mathbf{x}}_0^H \tilde{\mathbf{x}}_0, \tilde{\mathbf{x}}_0 = \hat{\mathbf{R}}_{\text{FP}}^{-1/2} \mathbf{x}_0, \tilde{\mathbf{S}} = \hat{\mathbf{R}}_{\text{FP}}^{-1/2} \mathbf{S}, \mathbf{P}_{\tilde{\mathbf{S}}} = \tilde{\mathbf{S}}(\tilde{\mathbf{S}}^H \tilde{\mathbf{S}})^{-1} \tilde{\mathbf{S}}^H, \mathbf{P}_{\tilde{\mathbf{S}}}^{\perp} = \mathbf{I}_N - \mathbf{P}_{\tilde{\mathbf{S}}}$.

B. ICBD-RAO subspace detector

In the Rao and Wald tests, we set $\boldsymbol{\theta} = [\boldsymbol{\theta}_r^T, \boldsymbol{\theta}_s^T]^T \in \mathbb{C}^{(t+1)\times 1}$, and we define $\boldsymbol{\theta}_r = \boldsymbol{\beta}$ and $\boldsymbol{\theta}_s = \tau$. The Rao test for the problem in (3) of the complex value is given by:

$$\left.\frac{\partial \ln f_1(\mathbf{x}_0|\boldsymbol{\theta})}{\partial \boldsymbol{\theta}_r}\right|_{\boldsymbol{\theta}=\hat{\boldsymbol{\theta}}_0}^{T} \left[\mathbf{I}^{-1}(\hat{\boldsymbol{\theta}}_0)\right]_{\boldsymbol{\theta}_r,\boldsymbol{\theta}_r} \left.\frac{\partial \ln f_1(\mathbf{x}_0|\boldsymbol{\theta})}{\partial \boldsymbol{\theta}_r^*}\right|_{\boldsymbol{\theta}=\hat{\boldsymbol{\theta}}_0} \underset{H_0}{\overset{H_1}{\lessgtr}} \zeta \tag{12}$$

where ζ denotes the detection threshold for the Rao test. $\hat{\boldsymbol{\theta}}_0$ denotes the ML estimate of $\boldsymbol{\theta}$ under H_0 hypothesis. $\mathbf{I}(\boldsymbol{\theta})$ is the Fisher information matrix (FIM), with the blocks of $\mathbf{I}_{\boldsymbol{\theta}_r,\boldsymbol{\theta}_r}(\boldsymbol{\theta})$, $\mathbf{I}_{\boldsymbol{\theta}_r,\boldsymbol{\theta}_s}(\boldsymbol{\theta})$, $\mathbf{I}_{\boldsymbol{\theta}_s,\boldsymbol{\theta}_r}(\boldsymbol{\theta})$, and $\mathbf{I}_{\boldsymbol{\theta}_s,\boldsymbol{\theta}_s}(\boldsymbol{\theta})$.

After some algebra, we yield

$$\frac{\partial \ln f_1(\mathbf{x}_0|\boldsymbol{\theta})}{\partial \boldsymbol{\theta}_r^T} = \frac{1}{\tau}(\mathbf{x}_0 - \mathbf{S}\boldsymbol{\beta})^H \mathbf{R}^{-1}\mathbf{S} \tag{13}$$

$$\frac{\partial \ln f_1(\mathbf{x}_0|\boldsymbol{\theta})}{\partial \boldsymbol{\theta}_r^*} = \frac{1}{\tau}\mathbf{S}^H \mathbf{R}^{-1}(\mathbf{x}_0 - \mathbf{S}\boldsymbol{\beta}) \tag{14}$$

We obtain the middle term of the Rao test in (12) by utilizing the matrix inversion lemma as follows:

$$\left[\mathbf{I}^{-1}\left(\hat{\boldsymbol{\theta}}_0\right)\right]_{\boldsymbol{\theta}_r,\boldsymbol{\theta}_r} = \tau(\mathbf{S}^H \mathbf{R}^{-1}\mathbf{S})^{-1} \tag{15}$$

The target is absent (i.e. $\boldsymbol{\beta} = \mathbf{0}_{t\times 1}$) under hypothesis H_0, the ML estimate of the relative parameter $\boldsymbol{\theta}_r$ is $\hat{\boldsymbol{\theta}}_r = \mathbf{0}_{t\times 1}$.

In the second step, we obtain the MAP estimate of the texture component τ as follows:

$$\hat{\tau}_0 = \arg\max_{\tau} f_0(\mathbf{x}_0|\tau) f(\tau) = \frac{\mu^2}{2\lambda}\left[-(2N+3) + \sqrt{(2N+3)^2 + \frac{4\lambda}{\mu^2}(\lambda + 2T_0)}\right] \tag{16}$$

Inserting (13), (14), (15),and the estimated speckle (16) into (12), the ICBD-based subspace detector by exploiting the Rao test in compound Gaussian sea clutter with inverse Gaussian texture (ICBD-RAO-IG) is given by:

$$\frac{2\lambda \tilde{\mathbf{x}}_0^H \mathbf{P}_{\tilde{\mathbf{S}}} \tilde{\mathbf{x}}_0}{\mu^2\left[-(2N+3) + \sqrt{(2N+3)^2 + \frac{4\lambda}{\mu^2}(\lambda + 2\hat{T}_0)}\right]} \underset{H_0}{\overset{H_1}{\gtrless}} \zeta \tag{17}$$

C. ICBD-WALD subspace detector

The Wald test of the complex value for the ICBD-based problem in (3) with known texture component and the speckle matrix is given by:

$$\hat{\boldsymbol{\theta}}_{r,1}^H \left\{\left[\mathbf{I}^{-1}(\hat{\boldsymbol{\theta}}_1)\right]_{\boldsymbol{\theta}_r,\boldsymbol{\theta}_r}\right\}^{-1} \hat{\boldsymbol{\theta}}_{r,1} \underset{H_0}{\overset{H_1}{\lessgtr}} \gamma \tag{18}$$

where γ denotes the detection threshold. $\hat{\boldsymbol{\theta}}_1$ and $\hat{\boldsymbol{\theta}}_{r,1}$ are the ML estimates of $\boldsymbol{\theta}$ and $\boldsymbol{\theta}_r$ under hypothesis H_1, respectively.

We take the derivative of the logarithm of (4), by setting the result equal to 0, and we yield the ML estimate of $\boldsymbol{\beta}$ in (7). Besides, we notice that the middle term is the inverse form of (15) as follows:

$$\left\{\left[\mathbf{I}^{-1}(\hat{\boldsymbol{\theta}}_1)\right]_{\boldsymbol{\theta}_r,\boldsymbol{\theta}_r}\right\}^{-1} = \frac{1}{\tau}\mathbf{S}^H \mathbf{R}^{-1}\mathbf{S} \tag{19}$$

Then, in the second step, we obtain the MAP estimate of the texture component τ under hypothesis H_1 as follows:

$$\hat{\tau}_1 = \arg\max_{\tau} f_1(\mathbf{x}_0|\tau) f(\tau) = \frac{\mu^2}{2\lambda}\left[-(2N+3) + \sqrt{(2N+3)^2 + \frac{4\lambda}{\mu^2}(\lambda + 2T_1)}\right] \tag{20}$$

Substituting (7), (19), and the estimated $\hat{\tau}_1$ and $\hat{\mathbf{R}}_{\text{FP}}$ into the test statistic of the Wald test in (18), after some algebra, we yield the ICBD-based subspace detector by exploiting the Wald test in compound Gaussian sea clutter with inverse Gaussian texture (ICBD-WALD-IG) as:

$$\frac{2\lambda \tilde{\mathbf{x}}_0^H \mathbf{P}_{\tilde{\mathbf{S}}} \tilde{\mathbf{x}}_0}{\mu^2\left[-(2N+3) + \sqrt{(2N+3)^2 + \frac{4\lambda}{\mu^2}(\lambda + 2\hat{T}_1)}\right]} \underset{H_0}{\overset{H_1}{\gtrless}} \gamma \tag{21}$$

IV. PERFORMANCE ASSESSMENT

In this section, we exploit the measured sea clutter data to exhibit the detection performance of the three subspace detectors. And we set $100/P_{fa}$ standard Monte Carlo experiments to obtain the detection threshold, where P_{fa} is the probability of false alarm. The probability of detection (i.e.P_d) is obtained by $10/P_{fa}$ experiments.

We define the signal-to-clutter ratio (SCR) as SCR (dB) = $10\log_{10}[\text{Tr}(\boldsymbol{\beta}^H \mathbf{H}^H \mathbf{H}\boldsymbol{\beta})/(N\mu)]$. The interference-to-clutter ratio (ICR) as ICR (dB) = $10\log_{10}[\text{Tr}(\boldsymbol{\varphi}^H \mathbf{J}^H \mathbf{J}\boldsymbol{\varphi})/(N\mu)]$.

We set $N = 12$, $K = 10$, $r = 2$, $p = 6$, $o = 4$, ICR = 20dB, and we generate the coordinate $\boldsymbol{\beta}'$ and $\boldsymbol{\varphi}'$ randomly.

Besides, we select the ICBD-GLRT-PHE, ICBD-RAO-HE, and ICBD-WALD-HE in [17] as the comparison detectors. Moreover, we set the ICBD-GLRT-IG, ICBD-RAO-IG, and ICBD-WALD-IG with known $\mathbf{R}$, which can not be obtained in the real situation, as benchmark.

A. Simulated Data

Fig. 1 shows the detection performance of the proposed detectors. Fig. 1(a) and Fig. 1(b) show the P_d versus SCR of the detectors. We can see that the proposed detectors achieve a gain of more than 3dB than the competitors in $P_d = 0.9$ in the

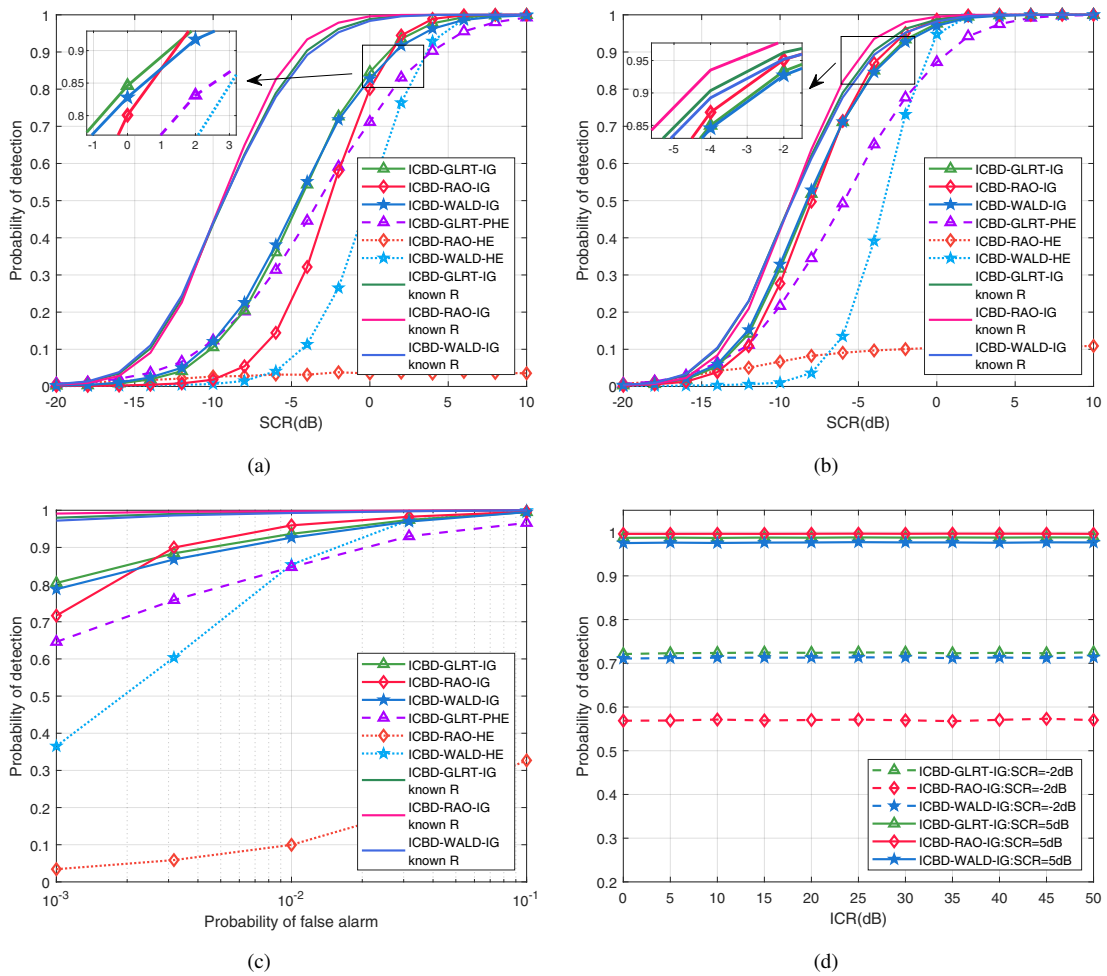

Fig. 1. Detection performance of the detectors in simulated sea clutter data. (a) P_d versus SCR in limited training data ($K = 10$). (b) P_d versus SCR in sufficient training data ($K = 24$). (c) ROC curves in SCR$= -2$dB. (d) P_d versus ICR in SCR$= -2$dB.

limited training data ($K = 10$) in Fig. 1(a). We set $K = 24$ in Fig. 1(b). We can observe that the detection performance of the novel detectors, which outperform the competitors, is close to the theoretical curves as the training data improves. In Fig. 1(c), we plot the ROC curves of the detectors. Fig. 1(c) shows the proposed detectors achieve higher P_d in a large range of P_{fa}. Fig. 1(d) is the P_d versus ICR curves of the newly detectors, which demonstrates the P_d remains unchanged as the ICR changes.

B. Real Sea Clutter Data

We select the IPIX radar file 86 [19] as the real sea clutter to verify the detection performance of the detectors. And we choose the 16-th range bin with HH polarization as the CUT. In the real sea clutter data, we define the signal-to-clutter ratio (SCR) as SCR (dB) $= 10\log_{10}(\sigma_t^2/\sigma_c^2)$, where the σ_t^2 and σ_c^2 represent the power of target and clutter, respectively. The interference-to-clutter ratio (ICR) as ICR (dB) $= 10\log_{10}(\sigma_i^2/\sigma_c^2)$, where the σ_i^2 represents the power of the interference.

In Fig. 2(a), we can see that the real sea clutter of high resolution radar is time varying. Fig. 2(b) is fitting result of the sea clutter and the estimated CG-IG distribution with $\mu = 1.983$ and $\lambda = 11.4656$. In Fig. 2(c), we set $K = 10$. It is observed that the novel detectors superior to the conventional detectors. Fig. 2(d) depicts the ROC curves of the detectors in SCR$=$10dB, and we find the proposed detectors achieve better detection performance than the competitors.

V. CONCLUSION

In conclusion, the target detection problem in IG-CG sea clutter with structured interference has been considered. We first exploit the ICBD-based method to transform the subspace detection problem. Then, we design three novel subspace detectors based on the two-step GLRT, Rao, and Wald tests. The experiment results demonstrate the proposed detectors outperform the conventional detectors.

REFERENCES

[1] Z. Wang, W. Liu, and H. Chen, *Adaptive Detection for Multichannel Signals in Non-Ideal Environments*. CRC Press, 2024.

[2] J.-P. Delmas, M. N. El Korso, S. Fortunati, and F. Pascal, *Elliptically symmetric distributions in signal processing and machine learning*. Springer, 2024.

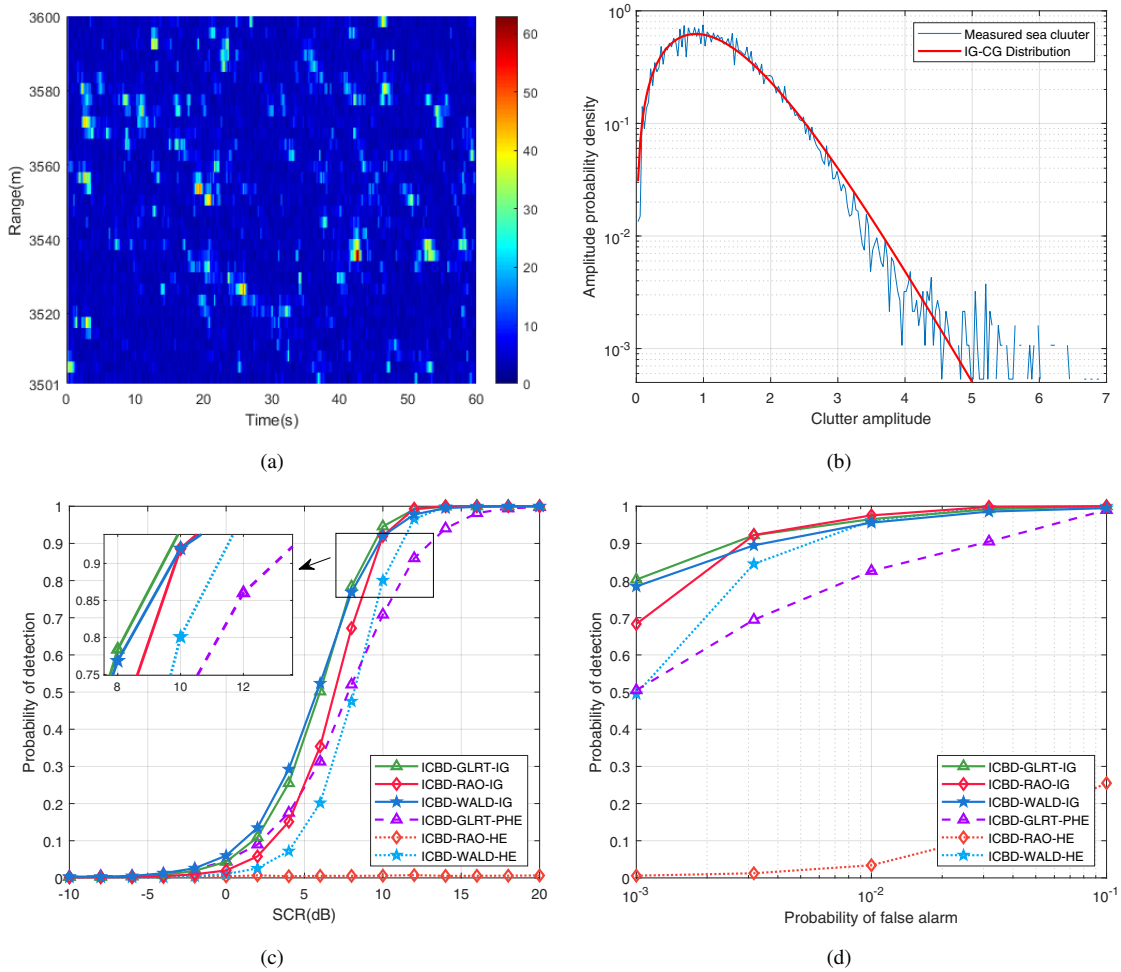

Fig. 2. Detection performance of the detectors in measured sea clutter data. (a) The real sea clutter. (b) Fitting result of 16-th range cell. (c) P_d versus SCR in $K = 10$. (d) ROC curves in SCR=10dB.

[3] F. C. Robey, D. R. Fuhrmann, E. J. Kelly, and R. Nitzberg, "A CFAR adaptive matched filter detector," *IEEE Trans. Aerosp. Electron. Syst.*, vol. 28, no. 1, pp. 208–216, 1992.

[4] L. L. Scharf and B. Friedlander, "Matched subspace detectors," *IEEE Trans. signal process.*, vol. 42, no. 8, pp. 2146–2157, 1994.

[5] J. Liu, S. Liu, W. Liu, S. Zhou, S. Zhu, and Z.-J. Zhang, "Persymmetric adaptive detection of distributed targets in compound-Gaussian sea clutter with Gamma texture," *Signal Process.*, vol. 152, pp. 340–349, 2018.

[6] Z. Wang, Z. He, Q. He, B. Xiong, and Z. Cheng, "Persymmetric adaptive target detection with dual-polarization in compound Gaussian sea clutter with inverse Gamma texture," *IEEE Trans. Geosci. Remote Sens.*, vol. 60, pp. 1–17, 2022.

[7] J. Xue, J. Liu, S. Xu, and M. Pan, "Adaptive detection of radar targets in heavy-tailed sea clutter with lognormal texture," *IEEE Trans. Geosci. Remote Sens.*, vol. 60, pp. 1–11, 2021.

[8] A. Mezache, F. Soltani, M. Sahed, and I. Chalabi, "Model for non-rayleigh clutter amplitudes using compound inverse Gaussian distribution: An experimental analysis," *IEEE Trans. Aerosp. Electron. Syst.*, vol. 51, no. 1, pp. 142–153, 2015.

[9] S. Xu, X. Shi, J. Xue, and P. Shui, "Adaptive subspace detection of range-spread target in compound Gaussian clutter with inverse Gaussian texture," *Digit. Signal Process.*, vol. 81, pp. 79–89, 2018.

[10] D. Ciuonzo, A. De Maio, and D. Orlando, "A unifying framework for adaptive radar detection in homogeneous plus structured interference—part II: Detectors design," *IEEE Trans. Signal Process.*, vol. 64, no. 11, pp. 2907–2919, 2016.

[11] A. De Maio and D. Orlando, "Adaptive radar detection of a subspace signal embedded in subspace structured plus Gaussian interference via invariance," *IEEE Trans. Signal Process.*, vol. 64, no. 8, pp. 2156–2167, 2015.

[12] Z. Wang, J. Liu, Y. Li, H. Chen, and M. Peng, "Adaptive subspace signal detection in structured interference plus compound Gaussian sea clutter," *Remote Sens.*, vol. 14, no. 9, p. 2274, 2022.

[13] G. Pailloux, P. Forster, J.-P. Ovarlez, and F. Pascal, "Persymmetric adaptive radar detectors," *IEEE Trans. Aerosp. Electron. Syst.*, vol. 47, no. 4, pp. 2376–2390, 2011.

[14] J. Xue, H. Li, M. Pan, and J. Liu, "Adaptive persymmetric detection for radar targets in correlated CG-LN sea clutter," *IEEE Trans. Geosci. Remote Sens.*, 2023.

[15] F. Bandiera, O. Besson, and G. Ricci, "Adaptive detection of distributed targets in compound-Gaussian noise without secondary data: a bayesian approach," *IEEE Trans. Signal Process.*, vol. 59, no. 12, pp. 5698–5708, 2011.

[16] I. P. Kirsteins and D. W. Tufts, "Adaptive detection using low rank approximation to a data matrix," *IEEE Trans. Aerosp. Electron. Syst.*, vol. 30, no. 1, pp. 55–67, 1994.

[17] W. Liu, J. Liu, T. Liu, H. Chen, and Y.-L. Wang, "Detector design and performance analysis for target detection in subspace interference," *IEEE Signal Process. Lett.*, 2023.

[18] F. Pascal, P. Forster, J.-P. Ovarlez, and P. Larzabal, "Performance analysis of covariance matrix estimates in impulsive noise," *IEEE Trans. Signal Process.*, vol. 56, no. 6, pp. 2206–2217, 2008.

[19] B. C. R. Bakker, "1998 McMaster IPIX radar sea clutter database," http://soma.mcmaster.ca/ipix.php.